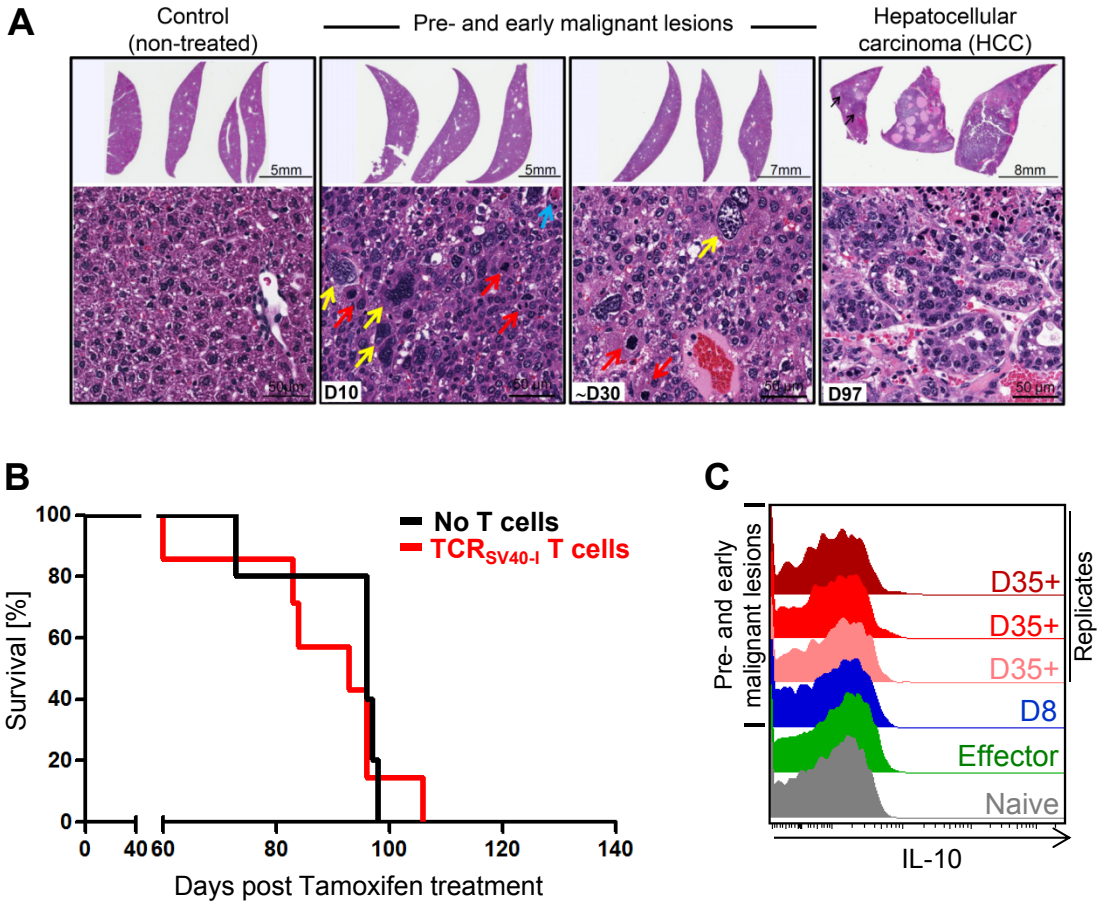

Supplemental Figure S1. Tumor-specific TCR_{SV40-I} CD8 T cells fail to control the development and progression of tamoxifen-induced liver tumors in ASTxCreER^{T2} mice, Related to Figure 1.

(**A**) Liver carcinogenesis in tamoxifen (Tam)-treated ASTxCre-ER^{T2} mice. Hematoxylin and Eosin staining of liver sections collected at indicated time points post Tam treatment; liver sections of non-treated ASTxCre-ER^{T2} mice are shown for comparison. At D10 and D34 cellular morphologic changes including karyomegaly, cytomegaly, multinucleated cells (yellow arrows), and an increase in mitotic figures (red arrows) are present, however the lobular architecture remains in tact and there is no evidence of hepatocellular adenoma, hepatocellular carcinoma (HCC), or inflammatory infiltrates; single cell necrosis (blue arrow). At D97 liver sections contain numerous malignant lesions/HCC (top panel) characterized by the absence of normal hepatic lobular architecture, prominent irregular trabeculae, and invasion into adjacent hepatic parenchyma (black arrows). See Materials and Methods for further description. (**B**) Kaplan-Meier survival analysis of Tam-treated ASTxCreER^{T2} mice that received $5x10^5$ naïve TCR_{SV40-I} (red; n=7); mice that received no T cells (black; n=5). *P* = 0.6517, log-rank test. (**C**) Dysfunctional tumor-specific TCR_{SV40-I} do not produce increased levels of the suppressor cytokine IL-10. D8 and D35 TCR_{SV40-I} were isolated from pre-/early malignant lesions, stimulated with peptide for 4.5 hours, and assessed for IL-10 production by intracellular cytokine staining. Data are representative of 2 independent experiments with n=3-4.

D8 PD-1 and PD-L1 blockade *in vivo*

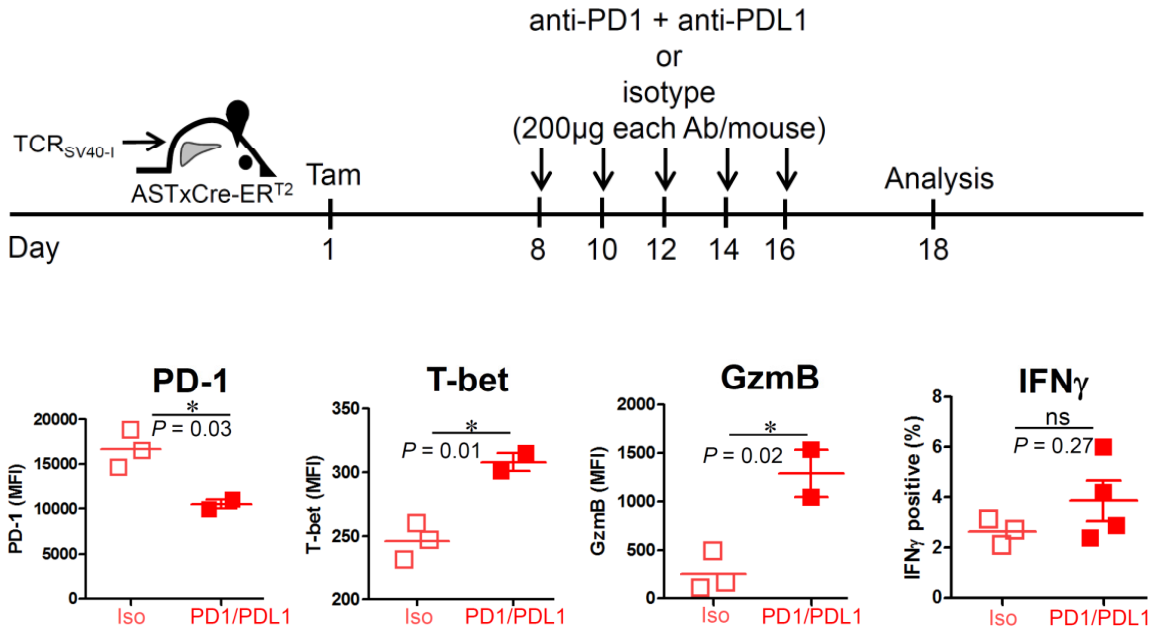

Supplemental Figure S2: Phenotypic and functional analyses of D8 TCR$_{SV40-I}$ after PD-1 and PD-L1 blockade *in vivo*. Related to Figure 2.

(Top) Experimental scheme, (bottom) flow cytometric analysis of TCR$_{SV40-I}$ isolated from liver lesions post checkpoint blockade; expression of PD-1, T-bet, Granzyme B, and IFNγ production (post 4.5h peptide stimulation) were assessed. Data show mean ± SEM; *P* values are shown. ns (= not statistically significant) using unpaired, two-tailed Student's *t* test (for analysis between isotype and treatment group). Each symbol represents an individual mouse.

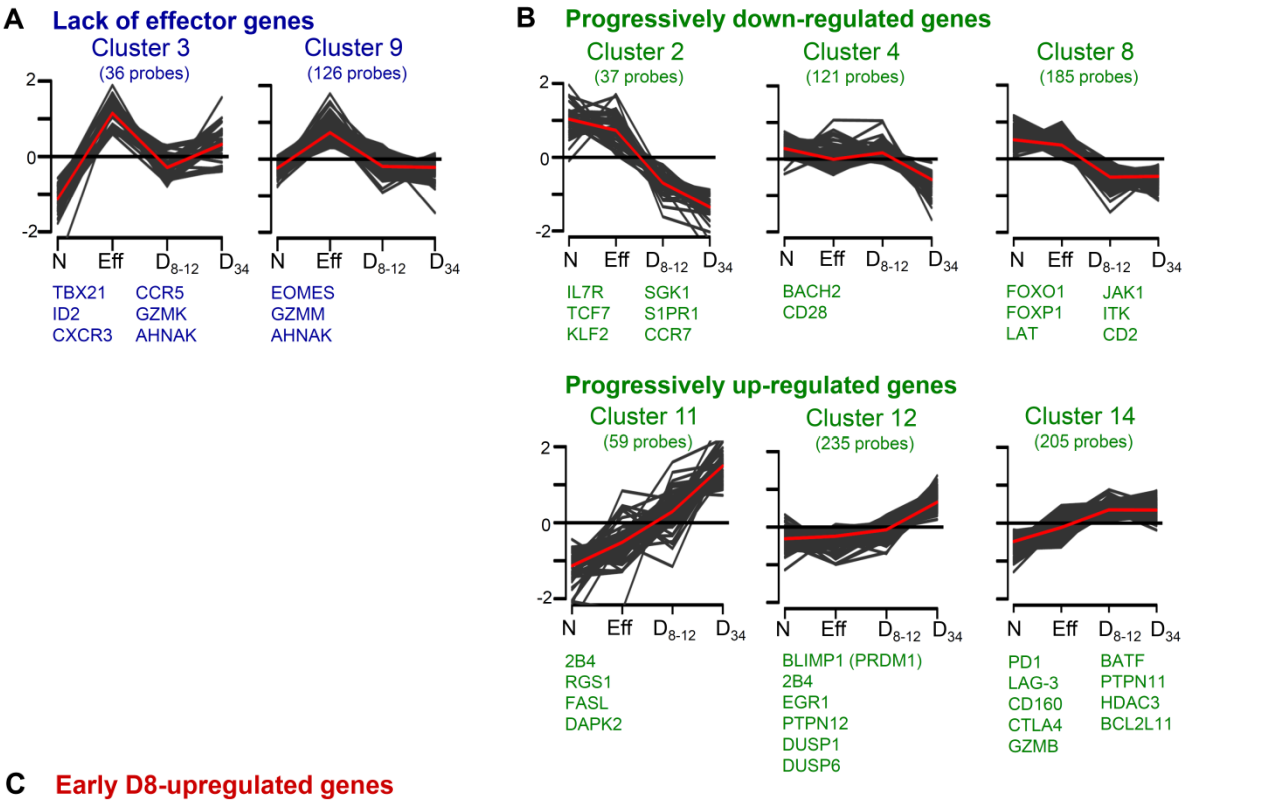

Supplemental Figure S3. K-means clustering of gene expression profiles from Naïve (N), D8-Effector (Eff) $TCR_{SV40\text{-}I}$, and D8-12 and D34 $TCR_{SV40\text{-}I}$ isolated from pre- and early malignant lesions, Related to Figure 3.

K-means clusters show log2-transformed expression intensities mean-centered at the probe-level. (**A**) Clusters 3 and 9 represent 'effector' genes that are not expressed in D8-12 and D34 $TCR_{SV40\text{-}I}$. (**B**) Clusters 2, 4, 8, and 11, 12, 14 represent genes that are progressively down- or up-regulated in D8-12 and D34 $TCR_{SV40\text{-}I}$. (**C**) Clusters 5 and 10 represent genes that are early expressed in D8-12 $TCR_{SV40\text{-}I}$.

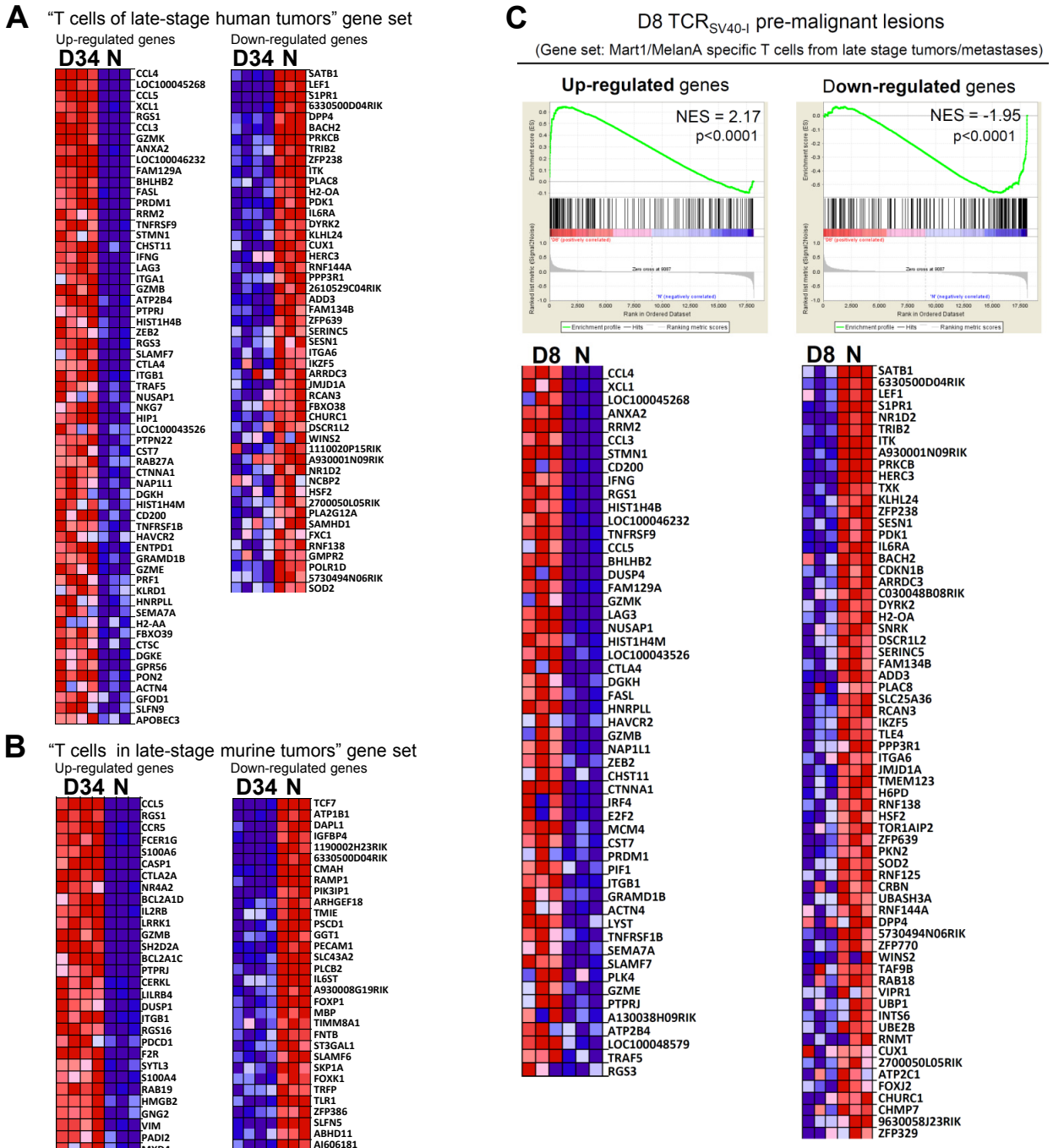

Supplemental Figure S4. D8- and D34-TCR$_{SV40-I}$ from pre- and early malignant lesions show enrichment of gene sets described for T cells isolated from late-stage/metastatic human and mouse tumors, Related to Figure 4.

Enrichment in D34-TCR$_{SV40-I}$ of genes previously shown to be differentially expressed in (**A**) human CD8 T cells isolated from metastatic lesions of melanoma patients (GSE24536), or (**B**) CD8 T cells isolated from established murine melanoma. (**C**) GSEA plot. Enrichment of genes in D8-TCR$_{SV40-I}$ found to be dysregulated in Mart1/MelanA CD8 T cells from late-stage/metastatic human tumors. NES, normalized enrichment score. Heat maps display genes with positive enrichment scores. Expression levels are represented as a gradient from high (red) to low (blue).

A

Exhaustion Gene Set

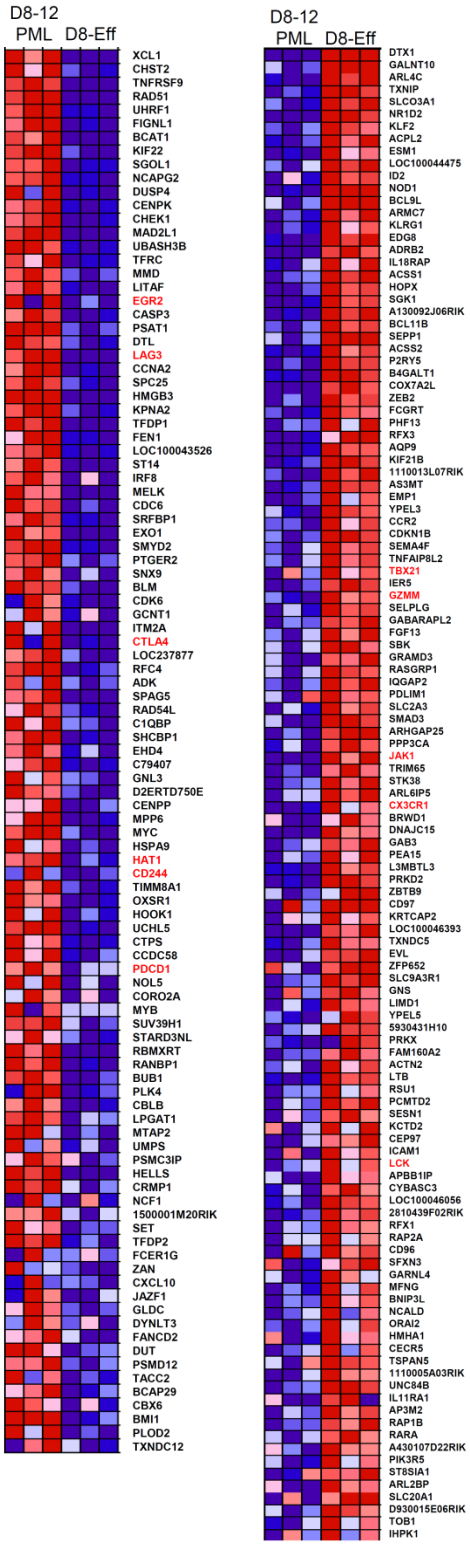

B

‘Up-regulated exhaustion genes’

IL21	ERMN
CDC27	SLC37A2
NDRG1	ART3
MTHFD2	SLC6A13
LOC100047490	ID3
SPOCK2	CCNB2
DDIT4	MYO1C
IPP	OPTN
RAD18	CUGBP2
CD160	RHOX8
GCSH	SKAP2
WDR67	PSPC1
XRCC2	GCA
PHLPP	NAT13
NEK2	SLC25A13
ETV5	HMGN3
BST2	BCL3
PWP1	CDC14A
UTP6	SPATS2
EIF1AY	KIFAP3
NRGN	GAS2
LAP3	FKBP5
RGS10	VAMP5
CPT1A	CCR9
HSH2D	AIM2
FABP5	INPP4B
SERPINE2	NAPSA
PCGF5	RSAD2
TARSL2	RNF128
NANP	TPD52
STAU2	RCSD1
CD109	IFITM3
PEX11A	CD83
LOC100044576	CD81
RTP4	ST6GAL1
PCTP	MEF2C

‘Down-regulated exhaustion genes’

ARHGEF2	VWA1
ABCG1	LOC100045268
CMA1	TKTL1
PIGB	5730593F17RIK
PRKAB2	MPND
IFNAR2	ATP2A3
LETM2	PRR13
RASL12	SLC12A7
MXD4	SYF2
PHF21A	WFIKKN2
ANXA4	TRAF3IP1
PLCG1	RRAS
UCKL1	PNPLA7
GTF2I	PGM2L1
SLC37A1	ITGB2
ABCA6	STAT6
PDCD6IP	TYK2
HSP105	STX17
FAM176B	FCGR2B
LRRC24	INSL6
PCDH21	BNIPL
SMOX	MKL1
GPX8	G0S2
1110036O03RIK	YES
TNIP1	KCNJ8
	RNF13

C

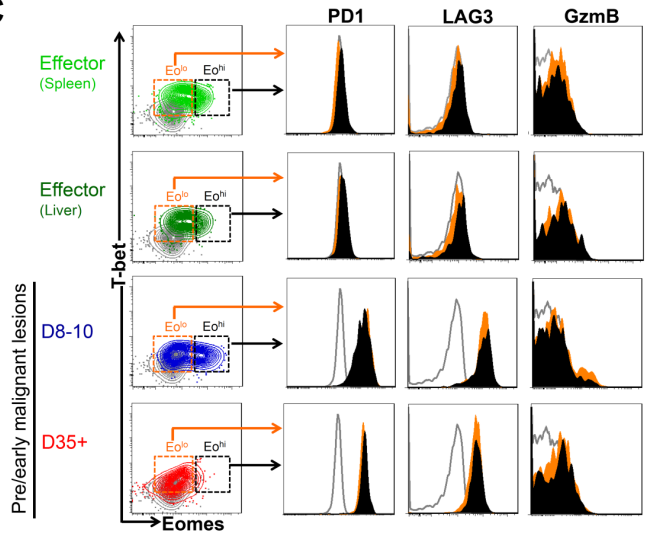

Supplemental Figure S5: Comparison between dysfunctional tumor-specific $TCR_{SV40\text{-}I}$ in pre- and early malignant lesions and exhausted T cells in chronic viral infections, Related to Figure 5.

(**A**) Gene set enrichment analysis of tumor-specific D8-12 $TCR_{SV40\text{-}I}$ from pre-malignant lesions (D8-12 PML) versus D8-Effectors during listeria infection (D8-Eff); applied was the 'D8-chronic viral infection/exhaustion' gene set (GSE30962; Broad Institute Molecular Signatures Database), which includes genes previously identified to be up- or down-regulated in virus-specific CD8 T cells at day 8 post chronic infection (versus virus-specific effector CD8 T cells at day 8 post acute infection).
(left) GSE30962_acute_vs_chronic_LCMV_primary_inf_cd8_Tcell_DN;
(right) (GSE30962_acute_vs_chronic_LCMV_primary_inf_cd8_Tcell_UP. Heat maps correspond to the gene set enrichment plots presented in Figure 5, displaying the expression levels of the 103 and 120 most enriched genes respectively. Expression levels are represented as a gradient from high (red) to low (blue). FDR *q* value $\leq$ 0.001. Some genes are highlighted in red as examples. (**B**) Genes that did not show significant enrichment in D8-PML T cells and did not receive a positive enrichment score. (**C**) Dysfunctional tumor-specific T cells lose Eomes expression over the course of tumor progression, and do not reveal differential GzmB, PD-1 and Lag-3 expression based on their relative Eomes expression levels. Representative T-bet and Eomes expression flow plots and representative histograms of GzmB, PD-1 or Lag-3 expression levels distinguished based on their relative $Eomes^{hi}$ (black) or $Eomes^{lo}$ (orange) expression levels; grey = Naïve T cells as control.

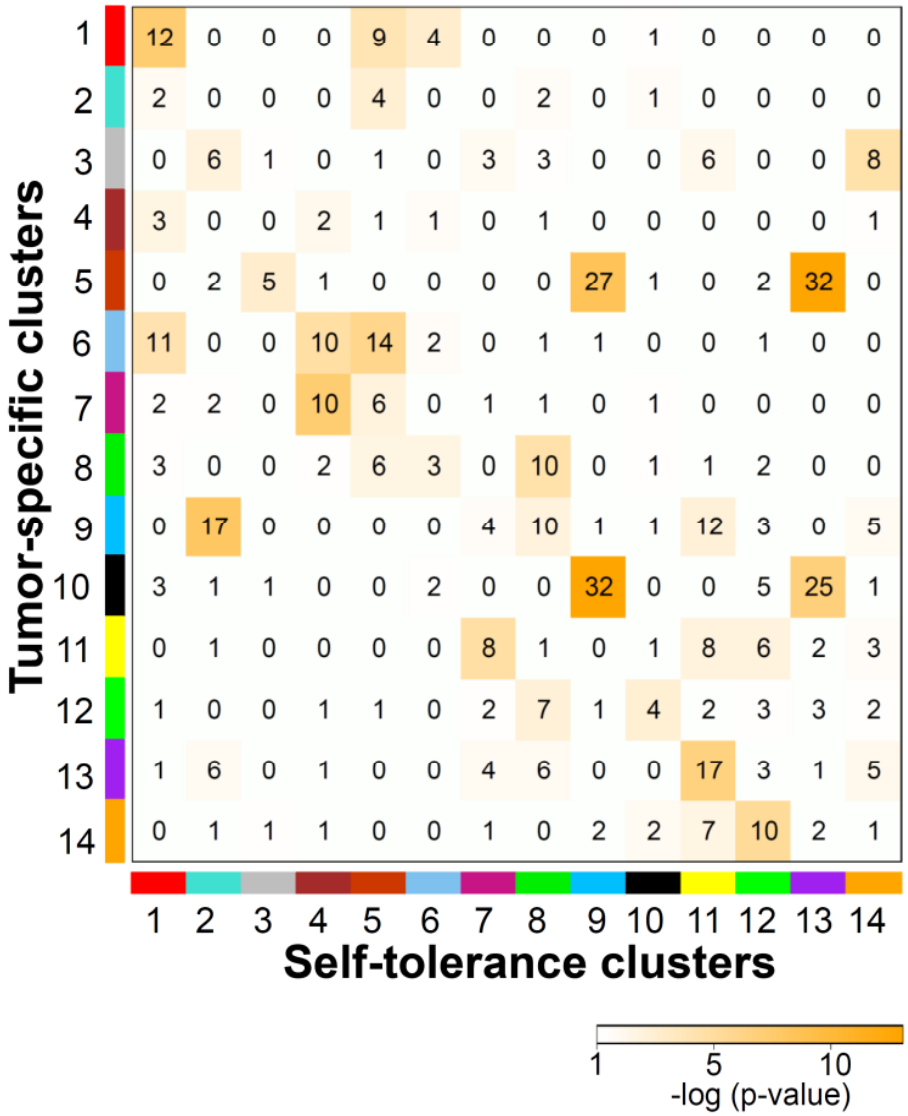

Supplemental Figure S6: Comparison of tumor-specific T cell dysfunction in pre-malignant lesions and self-tolerance, Related to Figure 3.

Gene expression signatures of $TCR_{SV40\text{-}I}$ CD8 T cells encountering tumor-specific antigen in pre-malignant lesions in livers, and self-tolerant TCR_{Gag} CD8 T cells encountering Gag self-antigen on normal hepatocytes were compared. Cross-tabulation comparing clusters from tumor-specific $TCR_{SV40\text{-}I}$ CD8 T cells (presented in Figures 3) with clusters from self-tolerant CD8 T cells previously described [Schietinger *et.al.*, Science (2012)]. Numbers show membership of overlapping genes between clusters. Color intensity scale reflects the $-\log_{10}$ p-value. Accompanied to this figure is Supplemental Table S3 listing genes from representative cluster overlaps.

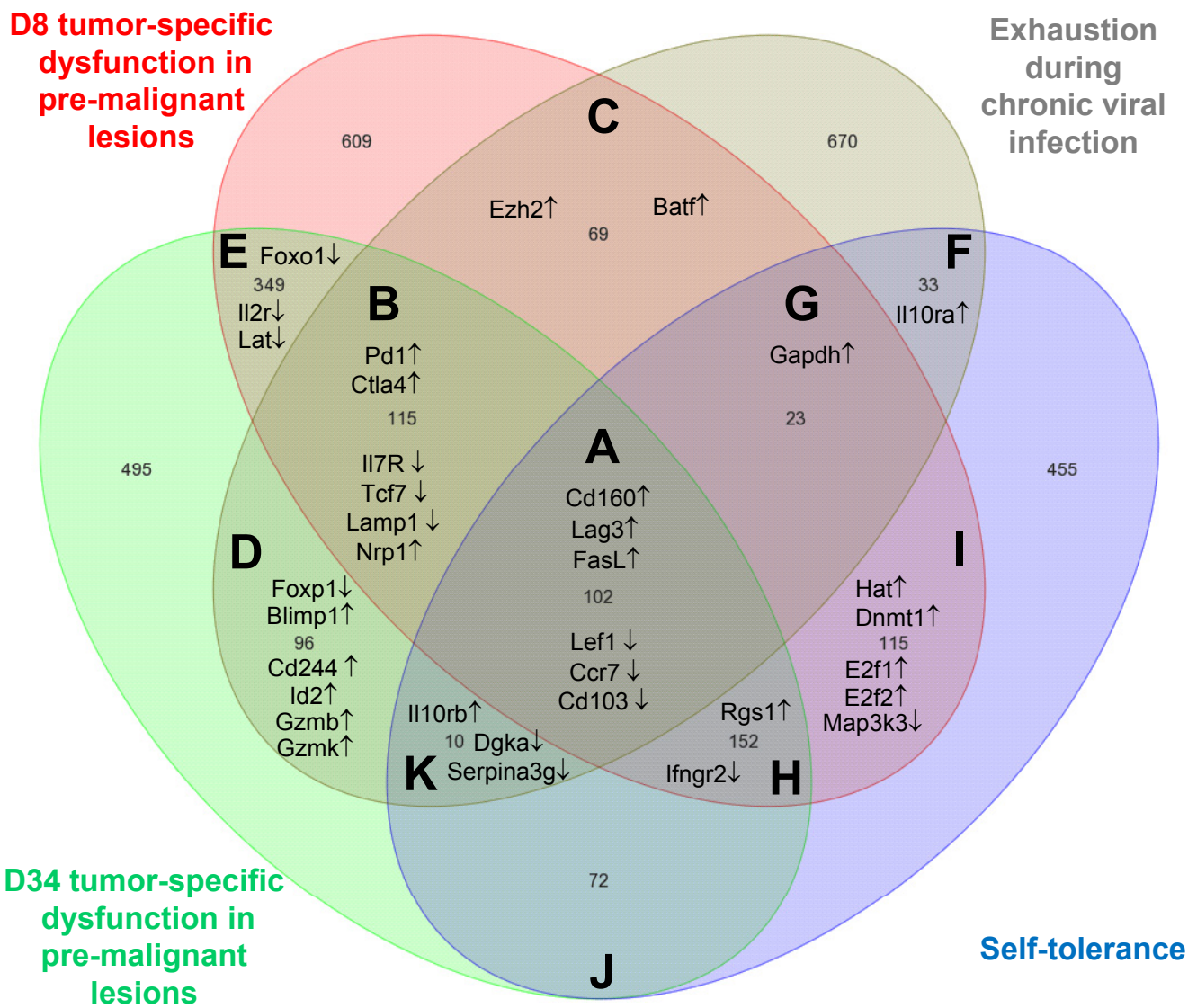

Supplemental Figure S7. Venn diagram of distinct states of CD8 T cell hyporesponsiveness, including tumor-specific T cell dysfunction in pre- and early malignant lesions, T cell exhaustion during chronic viral infection, and self-tolerance, Related to Figures 3 and 5.

Tumor-specific D8-$TCR_{SV40\text{-}I}$ (red), and D34-$TCR_{SV40\text{-}I}$ (green) CD8 T cells in pre- and early malignant lesions in livers (GSE60501), self-tolerant CD8 T cells (GSE32025), and exhausted virus-specific CD8 T cells during chronic viral LCMV clone 13 infection (Days 22-35) (GSE9650). Genes were normalized to naïve CD8 T cells present as a sample group in all data sets. Some genes are listed as examples. Accompanied to this figure is Supplemental Table S4 listing genes of all intersections.

SUPPLEMENTAL TABLES

Supplemental Table S1, related to Figure 3. **Genome-wide transcriptome analysis of tumor-specific TCR_{SV40-I} CD8 T cells in pre- and early malignant lesions.** List of differentially expressed genes in Naïve, Effector, D8- and D30+ TCR_{SV40-I}.

Supplemental Table S2, related to Figure 5. **Comparison between tumor-specific TCR_{SV40-I} from pre- and early malignant lesions and exhausted CD8 T cells in chronic infection.** List of genes found in each intersection of Venn-diagram displayed in Figure 5B.

Supplemental Table S3, related to Figure 3 and Supplemental Figure 6. **Comparison of tumor-specific T cell dysfunction and self-tolerance.** Genes from representative cluster overlaps. Column X (blue) lists previously characterized self-tolerance clusters. Column Y (green) lists "tumor-specific" clusters described in Figure 3.

Supplemental Table S4, related to Figures 3 and 5, and Supplemental Figure 7. **Comparison of tumor-specific TCR_{SV40-I}, exhausted T cells during chronic infection, or self-tolerance.** List of genes found in each intersection of Venn-diagram displayed in Supplemental Figure 7.

SUPPLEMENTAL EXPERIMENTAL PROCEDURS

Flow cytometric analysis

Flow cytometric analysis was performed using FACS Canto; cells were sorted using BD FACS Aria (BD Biosciences, San Jose, CA) at the Cell Analysis Facility, Department of Immunology, University of Washington, and Flow Facility at Memorial Sloan Kettering Cancer Center. Flow data were analyzed with FlowJo7.6 (Tree Star Inc, Ashland, OR).

Cell isolation for subsequent flow cytometric analyses including cell sorting

Mice were euthanized by cervical dislocation. Spleens were mechanically disrupted with the back of a 3-ml syringe, filtered through a 70-µm strainer, and red blood cells (RBC) were lysed with ammonium chloride potassium buffer. Cells were washed twice with cold RPMI 1640 media supplemented with 2µM glutamine, 100U/ml penicillin/streptomycin, and 5-10% FCS. Liver tissue was mechanically disrupted and dissociated with scissors (in 1-2ml of cold complete RPMI). Dissociated tissue pieces were transferred into a 70-µm strainer (placed into a 60mm dish with 1-2 ml of cold complete RPMI) and further dissociated with the back of a 3-ml syringe. Cell suspension was filtered through 70-µm strainers. RBCs were lysed with ammonium chloride potassium buffer.

Intracellular cytokine staining and CFSE labeling

Intracellular cytokine staining was performed using the Cytofix/Cytoperm Plus kit (BD Biosciences) per the manufacturer's instructions. Briefly, splenocytes or T cells from livers were mixed with $1\text{-}2x10^6$ congenically marked splenocytes and incubated with 0.5-0.75 µg/ml Tag-I peptide for 5 h at 37°C in the presence of GolgiPlug (brefeldin A). After staining for cell-surface molecules, the cells were fixed, permeabilized, and stained with antibodies to IFN-γ (XMG1.2) and TNF-α (MP6-XT22).

For measurement of cell proliferation *in vivo* naive TCR_{SV40-I} $CD8^+$ T cells were incubated with 10µM carboxyfluorescein succinimidyl ester (CFSE; Invitrogen) in serum-free HBSS for 15 min at 37°C. The

reaction was quenched with pure FCS and the cells were washed twice with serum-free RPMI medium before transfer into ASTxCre-ER^{T2} mice.

PD-1 and PD-L1 blockade in vivo

Anti-PD-1 (clone RMP1-14) and anti-PD-L1 (clone 10.F.9G2) antibodies, or isotype control (clone LTA-2) were purchased from BioXcell. Antibodies were given intraperitoneally at a dose of 200µg each per mouse at given time points as outlined in Figures 2F and S2.

Microarray sample preparation

Replicate samples were isolated from spleens or livers and sorted as follows:

(i) Naïve TCR$_{SV40-I}$ Thy1.1 T cells were sorted by flow cytometry (CD8$^+$/CD44^{lo}) from spleens of TCR$_{SV40-I}$ Thy1.1 transgenic mice.

(ii) Effector TCR$_{SV40-I}$ Thy1.1 T cells were sorted by flow cytometry (CD8$^+$/Thy1.1$^+$) from spleens of infected B6 (Thy1.2) host mice (see above) 8 days post listeria infection.

(iii) D8-12 TCR$_{SV40-I}$: naïve TCR$_{SV40-I}$ Thy1.1 T cells were adoptively transferred into ASTxCre-ER^{T2} mice. 1-2 days later, mice were given 1mg tamoxifen i.p. 8-12 days post tamoxifen induction, T cells were isolated and sorted (CD8$^+$/Thy1.1$^+$) from livers as described above.

(iii) D34 TCR$_{SV40-I}$: naïve TCR$_{SV40-I}$ Thy1.1 T cells were adoptively transferred into ASTxCre-ER^{T2} mice. 1-2 days later, mice were given 1mg tamoxifen i.p. 31-34 days post tamoxifen induction, T cells were isolated and sorted (CD8$^+$/Thy1.1$^+$) from livers as described above.

After flow sort, cells were washed twice with cold PBS and cell pellets were frozen and stored at -80°C. RNA was isolated using Qiagen RNeasy Plus Micro and Qiagen RNeasy Plus Mini Kits per the manufacturer's instructions and the yield was determined on a Qubit® 2.0 Fluorometer (Life Technologies, Grand Island, NY). Samples were subsequently analyzed for RNA integrity using an Agilent 2200 TapeStation (Agilent Technologies, Inc., Santa Clara, CA). RNA that was determined to be of high quality (RINe ≥ 6.5) was amplified using the Ovation® PicoSL WTA System V2 (NuGEN Technologies, Inc., San Carlos, CA), biotin labeled using the Encore® BiotinIL Module (NuGEN Technologies, Inc., San Carlos, CA), and subsequently processed on a MouseRef-8 v2.0 Expression BeadChip (Illumina, Inc., San Diego, CA). Sample labeling, hybridization, scanning, and data acquisition were performed by the Genomics Shared Resource at the Fred Hutchinson Cancer Research Center.

Microarray data analysis

The complete dataset consisting of all arrays was processed using the Bioconductor package *lumi* by employing quantile normalization (Du et al., 2008). The dataset was initially filtered by flagging probes that were below a defined signal "noise floor," which was calculated as the 75th percentile of the negative control probe signals within each array. For each pair-wise comparison (for significance testing and k-means clustering; using naïve as the reference), a probe was retained if all of the samples in at least one condition were not flagged by the intensity filter. We further filtered each pair-wise comparison through the application of a variance filter, using the "shorth" function from the Bioconductor package *genefilter*. Differential gene expression was determined using the Bioconductor package *limma* (Smyth, 2005), and a false discovery rate (FDR) method was used to correct for multiple testing (Reiner et al., 2003). Significant differential gene expression was defined as $|\log_2(\text{ratio})| \geq 0.585$ (± 1.5-fold) and FDR ≤ 0.05. K-means cluster analysis was performed for those genes found to be differentially expressed in one or more comparison. The normalized $\log_2$ signal intensities were mean-centered at the probe-level and replicate samples were averaged prior to clustering. The number of clusters was selected using the figure of merit (FOM) method (Yeung et al., 2001). K-means clustering and cluster number estimation were performed using the TM4 microarray software suite MultiExperimental Viewer (MeV) (Saeed et al., 2003). Principal component analysis (PCA) plots were generated using R (Team, 2014). Overrepresented GO Biological Process terms comprised of genes found in clusters 5 and 10 were identified using a standard

hypergeometric test in the Bioconductor package GOstats (Falcon and Gentleman, 2007). In the hypergeometric tests, the gene list used as input was comprised of probe identifiers with Entrez Gene IDs from clusters 5 and 10, against a 'universe' comprised of all genes represented on the array. Gene set enrichment analysis (GSEA; http://www.broadinstitute.org/gsea) was used to determine whether predefined gene sets showed enrichment in T cell sample groups "D8 $TCR_{SV40\text{-}I}$" versus "Effectors" (Mootha et al., 2003; Subramanian et al., 2005). The following 2 gene sets from the Broad Institute Molecular Signatures Database were used: GSE30962_acute_vs_chronic_LCMV_primary_inf_cd8_Tcell_DN, and GSE30962_acute_vs_chronic_LCMV_primary_inf_cd8_Tcell_UP. Statistical significance was determined by permutation testing with NES (= normalized enrichment score).
The R package WGCNA was used to generate overlap numbers and probabilities between the tumor-specific and self-tolerant cluster sets. The Venn diagram was generated using Partek® Genomics Suite® software, version 6.6 Copyright ©; 2014 Partek Inc., St. Louis, MO, USA. A threshold of $|\log_2 (\text{ratio})| \geq 0.585$ (± 1.5-fold) and FDR ≤ 0.05 was used to select significant probes in each of the comparisons. The microarray data have been deposited in the Gene Expression Omnibus with accession code GSE60501.

Microarray data from Baitsch *et al.* (Baitsch et al., 2011), generated on the Agilent Whole Human Genome Microarray 4x44K platform, was downloaded from GEO (GSE24536), and Feature Extraction files were imported into R using the Bioconductor package limma (Smyth, 2005) to facilitate the comparison between tumor TILN and tumor PBMC samples. Replicate samples and a single outlier detected by PCA were discarded from downstream analysis. Replicate probes were averaged and the data quantile normalized. Filtering was performed such that for a given gene to be retained, at least 70% of the samples from at least one group had to be flagged as 'well above background.' The data was further filtered through the application of a variance filter, using the "shorth" function from the Bioconductor package genefilter. Differential gene expression was determined using the Bioconductor package limma, and a false discovery rate (FDR) method was used to correct for multiple testing. Significant differential gene expression was defined as |log2 (ratio)| ≥ 0.585 (± 1.5-fold) and FDR ≤ 0.05. For GSEA, significantly differentially expressed probes from the Agilent platform were mapped to Illumina MouseRef8v2 probes identifiers using BioMart.

Microarray data from Giordano *et al.* (Giordano et al., 2015), generated on the Agilent SurePrint G3 Mouse GE 8x60K platform, was downloaded from GEO (GSE42824), and Feature Extraction files were imported into R using the Bioconductor package limma (Smyth, 2005) to facilitate the comparison between TILs and untreated CD8 T cell samples. Replicate probes were averaged and the data quantile normalized. Filtering was performed such that for a given gene to be retained, at least 3 samples from at least one group had to be flagged as 'well above background.' The data was further filtered through the application of a variance filter, using the "shorth" function of the Bioconductor package genefilter. Differential gene expression was determined using the Bioconductor package limma, and a false discovery rate (FDR) method was used to correct for multiple testing. Significant differential gene expression was defined as |log2 (ratio)| ≥ 0.585 (± 1.5-fold) and FDR ≤ 0.05. For GSEA, significantly differentially expressed probes from the Agilent platform were mapped to Illumina MouseRef8v2 probes identifiers using BioMart (Smedley et al., 2015).

Histology

Micro-dissected liver tissues were fixed in 10% neutral buffered formalin, embedded in paraffin, and cut into 4-µm sections for hematoxylin and eosin (H&E) staining. H&E staining of paraffin sections was performed according to standard procedures. Tissues were processed by the Experimental Histopathology Core at the Fred Hutchinson Cancer Research Center (Seattle, WA). Images were captured from whole-slide images acquired with Aperio ScanScore AT (Leica Biosystems) using 40x

objectives. Sections were reviewed by board certified pathologist S.E.K. Pre- and early malignant lesions and HCC tumors in livers were classified based on published descriptions (Cullen et al., 1993; Deschl et al., 2001; Thoolen et al., 2010).

Statistical analyses

Statistical analyses were performed using unpaired two-tailed Student's *t* tests (Prism version 5.0, GraphPad Software), or Mann-Whitney U-tests as indicated. A *P* value of <0.05 was considered statistically significant. Survival studies were assessed by Kaplan-Meier curves and the log-rank (Mantel-Cox) test.

SUPPLEMENTAL REFERENCES

Baitsch, L., Baumgaertner, P., Devevre, E., Raghav, S.K., Legat, A., Barba, L., Wieckowski, S., Bouzourene, H., Deplancke, B., Romero, P.*, et al.* (2011). Exhaustion of tumor-specific CD8 T cells in metastases from melanoma patients. J Clin Invest *121*, 2350-2360.

Cullen, J.M., Sandgren, E.P., Brinster, R.L., and Maronpot, R.R. (1993). Histologic characterization of hepatic carcinogenesis in transgenic mice expressing SV40 T-antigens. Vet Pathol *30*, 111-118.

Deschl, U., Cattley, R., Harada, T., Kuttler, K., Hailey, J., Hartig, F., Leblanc, B., Marsman, D.S., and Shirai, T. (2001). Liver, gallbladder and exocrine pancreas. In International Classification of Rodent Tumors: the mouse, U. Mohr, ed. (Heidelberg, Germany: Springer Verlag), pp. 59–86.

Du, P., Kibbe, W.A., and Lin, S.M. (2008). lumi: a pipeline for processing Illumina microarray. Bioinformatics *24*, 1547-1548.

Falcon, S., and Gentleman, R. (2007). Using GOstats to test gene lists for GO term association. Bioinformatics *23*, 257-258.

Giordano, M., Henin, C., Maurizio, J., Imbratta, C., Bourdely, P., Buferne, M., Baitsch, L., Vanhille, L., Sieweke, M.H., Speiser, D.E.*, et al.* (2015). Molecular profiling of CD8 T cells in autochthonous melanoma identifies Maf as driver of exhaustion. EMBO J. *34*, 2042-58.

Mootha, V.K., Lindgren, C.M., Eriksson, K.F., Subramanian, A., Sihag, S., Lehar, J., Puigserver, P., Carlsson, E., Ridderstrale, M., Laurila, E.*, et al.* (2003). PGC-1alpha-responsive genes involved in oxidative phosphorylation are coordinately downregulated in human diabetes. Nat Genet *34*, 267-273.

Reiner, A., Yekutieli, D., and Benjamini, Y. (2003). Identifying differentially expressed genes using false discovery rate controlling procedures. Bioinformatics *19*, 368-375.

Saeed, A.I., Sharov, V., White, J., Li, J., Liang, W., Bhagabati, N., Braisted, J., Klapa, M., Currier, T., Thiagarajan, M.*, et al.* (2003). TM4: a free, open-source system for microarray data management and analysis. Biotechniques *34*, 374-378.

Smedley, D., Haider, S., Durinck, S., Pandini, L., Provero, P., Allen, J., Arnaiz, O., Awedh, M.H., Baldock, R., Barbiera, G.*, et al.* (2015). The BioMart community portal: an innovative alternative to large, centralized data repositories. Nucleic Acids Res *43*, W589-598.

Smyth, G.K. (2005). Limma: linear models for microarray data. In: Bioinformatics and Computational Biology Solutions using R and Bioconductor. In, V.C. R. Gentleman, S. Dudoit, R. Irizarry, W. Huber, ed. (New York: Springer), pp. 397–420.

Subramanian, A., Tamayo, P., Mootha, V.K., Mukherjee, S., Ebert, B.L., Gillette, M.A., Paulovich, A., Pomeroy, S.L., Golub, T.R., Lander, E.S.*, et al.* (2005). Gene set enrichment analysis: a knowledge-based approach for interpreting genome-wide expression profiles. Proc Natl Acad Sci U S A *102*, 15545-15550.

Team, R.D.C. (2014). R: A Language and Environment for Statistical Computing. In R Foundation for Statistical Computing (Vienna, Austria).

Thoolen, B., Maronpot, R.R., Harada, T., Nyska, A., Rousseaux, C., Nolte, T., Malarkey, D.E., Kaufmann, W., Kuttler, K., Deschl, U.*, et al.* (2010). Proliferative and nonproliferative lesions of the rat and mouse hepatobiliary system. Toxicol Pathol *38*, 5S-81S.

Yeung, K.Y., Haynor, D.R., and Ruzzo, W.L. (2001). Validating clustering for gene expression data. Bioinformatics *17*, 309-318.